Hindawi
Advances in Materials Science and Engineering
Volume 2021, Article ID 9579453, 19 pages
https://doi.org/10.1155/2021/9579453

Research Article

A PID Tuning Strategy Based on a Variable Weight Beetle Antennae Search Algorithm for Hydraulic Systems

Yujing Qiao[1] **and Yuqi Fan**[2]

[1]*School of Mechanical Engineering, Yangzhou Polytechnic College, Yangzhou 225009, China*
[2]*School of Mechanical Power Engineering, Harbin University of Science and Technology, Harbin 150000, China*

Correspondence should be addressed to Yujing Qiao; qiaoyujing@sina.com

Received 26 June 2021; Revised 10 August 2021; Accepted 19 August 2021; Published 15 September 2021

Academic Editor: Francisco Javier Fernández Fernández

To select reasonable PID controller parameters and improve control performances of hydraulic systems, a variable weight beetle antenna search algorithm is proposed for PID tuning in the hydraulic system. The beetle antennae search algorithm is inspired by the beetle preying habit depending on symmetry antennae on the head. The proposed algorithm added the exponential equation mechanism strategy in the basic algorithm to further improve the searching performance, the convergence speed, and the optimization accuracy and obtain new iteration and an updating method in the global searching and local searching stages. In the PID tuning process, advantages of less parameters and fast iteration are realized in the PID tuning process. In this paper, different dimension functions were tested, and results calculated by the proposed algorithm were compared with other famous algorithms, and the numerical analysis was carried out, including the iteration, the box-plot, and the searching path, which comprehensively showed the searching balance in the proposed algorithm. Finally, the reasonable PID controller parameters are found by using the proposed method, and the tuned PID controller is introduced into the hydraulic system for control, and the time-domain response characteristics and frequency response characteristics are given. The results show that the proposed PID tuning method has good PID parameter tuning ability, and the tuned PID has a good control ability, which makes the hydraulic system achieve the desired effect.

1. Introduction

Hydraulic systems, as an important transmission form in the traditional industry, are widely used in various heavy industries, military equipment and engineering vehicles [1–8], which is a high-level signal response closed-loop system. Because the hydraulic system is the time-varying, there are nonlinear and external interferences, uncertain system parameters, and cross load oscillations, and the bandwidth is also required. Under different requirements of the high precision, the fast speed, and the tracking ability, the hydraulic system controller affects the working accuracy in the system [9–11]. Therefore, the dynamic stability, the responsiveness, and the static control accuracy in the hydraulic system are problems that researchers have been concerned about.

There are many control methods, such as the nonlinear model predictive control, the robust control, and the adaptive control [12–14]. The traditional PID control strategy can complete the automatic control, but it has some shortcomings in the control precision and quality. It is difficult to overcome the nonlinear and uncertain parameters in the hydraulic system. PID parameters affect the dynamic performance of the controlled system, so it is very important to choose a reasonable PID tuning method [15–17].

With the rapid development of the electronic information technology and the wide application of intelligent control algorithm, a series of advanced new PID control strategies, such as the neural network PID, the robust nonfragile PID, the fuzzy PID, the sliding mode variable structure PID, and the adaptive PID, are born. Although these control algorithms have some advantages, it is difficult to realize in the actual control process. When the system has a large uncertainty, it cannot meet the control performance requirements of electrohydraulic servo control system in terms of the transient response. In recent years, the metaheuristic algorithm has been widely used in the field of

engineering for its advantages of simple implementation, wide application, and strong practicability. It shows a good performance in solving linear and nonlinear problems, constraint functions, multiobjective problems, and so on [18–20]. The intelligent algorithm is used to adjust PID parameters, such as future search algorithm, fireworks algorithm, particle swarm optimization algorithm, and crow search algorithm, which greatly improves the PID control performance [21–24]. The beetle antennae search algorithm (BAS) inspired by beetle living habits was proposed by Jiang and Li in 2017 [25]. The beetle preying habit in nature depends on the symmetry antennae on both sides of the beetle head, and antennae odor cells can find the concentration of food pheromone in the air. BAS is the metaheuristic algorithm with symmetry properties. Because symmetry antennae odor cells can sense the concentration difference between two directions, the beetle will move one side which has a stronger concentration, thereby continuously updating the beetle position. BAS has not only recognition and symmetry abilities. Compared with traditional algorithms, BAS has highly competitive. For PSO, BAS owns a strong jumping ability and a faster convergence speed. GA has a lot of computation because of the binary coding. BAS has less initial parameters than FA algorithm, so it is less affected by parameter sensitivity than FA. The core code in BAS is very short, only four lines, and it is easy to be implement in the computer. For BA and artificial bee colony (ABC), BAS owns a higher efficiency and lower complexity [26, 27] and is used in many fields [28–37].

According to the beetle living habits, the BAS searching steps mainly rely on two manual selection parameters including the orientation and the step size. BAS having the appropriate orientation parameter and the step size parameter can ensure a large searching scope and a fast convergence speed in all searching stages. However, parameters selected by artificial experiences are blind and random, and unreasonable parameters can limit BAS searching efficiencies. To further enhance the BAS optimization abilities, this paper proposed the variable weight beetle antennae search algorithm (VWBAS) which added the exponential equation in basic BAS. VWBAS can increase searching production, reduce labor costs, avoid falling into locally feasible solutions. To further enhance the BAS searching abilities and strengthen the PID control performances in hydraulic systems, this paper used the proposed algorithm to tune PID parameters in hydraulic systems.

The rest of this paper is organized as follows: in Section 2, the basic hydraulic system model was established. In Section 3, the proposed VWBAS was described. In Section 4, ten benchmark functions were given, and experiment results were discussed. In Section 5, the PID tuning method was proposed. In Section 6, different response analyses in the hydraulic system were discussed.

2. Hydraulic System Model

The basic structure of the hydraulic actuator system in this paper is composed of the servo valve, a servo amplifier, the hydraulic cylinder, the link mechanism, the sensor, and the spring. The sensor is linked by the elastic connection. Other parts are linked by the rigid connection. The simplified model is shown in Figure 1. The servo valve can output the modulated flow and the pressure after receiving the electrical analog signal and can convert the weak electrical signal into strong hydraulic energy. The servo valve will be input into the electric current signal changed by the voltage signal. Then, the electric current signal will drive the slide valve, and the slide valve will draw and stretch the piston rod in the hydraulic cylinder. Finally, the signal will be input into the controller to control the system by the conversion element. In Figure 1, Q_1 (m^3/s) means the inlet oil flow in the servo valve inlet. Q_2 (m^3/s) means the return oil flow in the servo valve. P_1 (Pa) means the working loads in the rodless cavity. P_2 (Pa) means the working loads in the rod cavity. B_P (N/(m/s)) means the viscous damping coefficient. K (kN/m) denotes the spring stiffness. A (m^2) is the piston area.

When Q_1 (m^3/s) and Q_2 (m^3/s) flow in the servo valve, the force F (N) will be compensated by the load pressure drop p_L (Pa) in the hydraulic cylinder:

$$\begin{aligned} Q_1 &= A\dot{y} + C_{ip}(P_1 - P_2) + C_{ep}P_1 + \frac{V_1 + Ay}{\beta_e}\dot{P}_1, \\ Q_2 &= A\frac{\mathrm{d}y}{\mathrm{d}t} + C_{ip}(P_1 - P_2) - C_{ep}P_2 - \frac{V_2 - Ay}{\beta_e}\dot{P}_2, \end{aligned} \tag{1}$$

where β_e ($N/(m^2.pa)$) is the oil effective bulk modulus, V_1 (m^3) is the initial oil cavity volume, V_2 (m^3) is C_{ip} ($m^3/(s.pa)$) is the internal leakage coefficient, C_{ep} ($m^3/(s.pa)$) is the external leakage coefficient, and the initial oil-out cavity volume and the initial oil-in cavity have the same volume, so the linearized load flow can be expressed as:

$$Q_L = K_q x_v - K_c p_L, \tag{2}$$

where x_v (m) means the spool displacement of the main valve, K_q (m^2/s) means the flow gain coefficient, and K_c ($m^5/(N{\cdot}s)$) is flow pressure coefficient:

$$\begin{aligned} K_q &= \frac{\partial}{\partial}\frac{Q_L}{x_v} = C_d w\sqrt{\frac{p_s - p_L}{\rho}}, \\ K_c &= \frac{\partial}{\partial}\frac{Q_L}{p_L} = \frac{C_d w x_v\sqrt{(p_s - p_L)/\rho}}{2(p_s - p_L)}, \end{aligned} \tag{3}$$

where C_d ($m^3/(s.pa)$) means the discharge coefficient, p_s (Pa) means the inlet oil pressure, p_o (Pa) means the return oil pressure, w_v (m) means the constant area gradient, and ρ (kg/m^3) is the hydraulic oil density.

The load flow rate continuity is given by

$$Q_L = A\dot{y} + C_{tp}p_L + \frac{V\dot{p}_L}{(4\beta_e)}, \tag{4}$$

where C_{tp} ($m^5/(N{\cdot}s)$) is the total leakage coefficient, and V (m^3) is the total volume of the cavity. The dynamic characteristic of hydraulic systems will be affected by the loading performance. Loading forces include the inertial force, the viscous damping force, the elastic force, and the extra force. The force equilibrium equation of the piston is given by

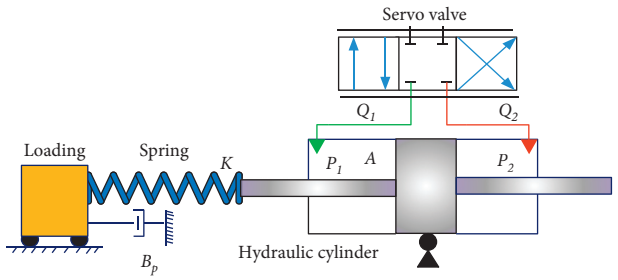

Figure 1: The hydraulic system simplified model.

$$Ap_L = M\ddot{y} + B_p p_L + \frac{V\dot{p}_L}{(4\beta_e)}, \tag{5}$$

where y (m) is the displacement of the piston, M (kg) is the total equivalent mass referred to the piston. When the piston is in the middle position, the liquid compression influence is the biggest, and the natural frequency of hydraulic components is the lowest, and the damping ratio is the smallest, and the stability of the system is the worst. So, the middle position of the piston should be taken as the initial position in the analysis of the hydraulic system. The block diagram of the hydraulic cylinder displacement can be given in Figure 2 by the loading pressure. And the block diagram can be used for the simulation analysis when the loading inertia and the leakage coefficient are large, and the dynamic procedure is slow.

3. A Variable Weight Beetle Antennae Search Algorithm

3.1. Beetle Antennae Search Algorithm. BAS is a new metaheuristic algorithm inspired by the detection and searching abilities of beetles. Two long antennae of one beetle usually contain many odor-receiving cells that can detect the odor for obtaining the sex pheromone of the potential suitable mate. So, beetles find food by their antennae. If the left antennae receive an odor that is stronger than another antenna, the beetle will fly to the left position; otherwise, it will fly to the right position. The beetle can find food effectively through the easy principle. In BAS, the best value of the objective function can be seen as food, and the variable of the objective function can be regarded as the beetle position. In nature, beetles usually randomly search for food in unknown regions. So, BAS uses the following formula to generate a random direction to simulate searching behavior:

$$\vec{b} = \frac{|\mathrm{rnd}(D,1)|}{\|\mathrm{rnd}(D,1)\|}, \tag{6}$$

where rnd means the random function giving a random vector in D dimension searching space. After a beetle determines the head direction, the beetle will move next positions by the odor intensity of two antennae. Left and right antennae positions can be generated as follows:

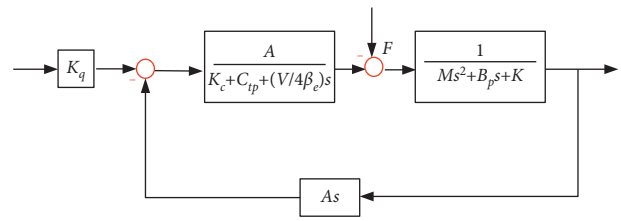

Figure 2: The hydraulic system block diagram.

$$\begin{cases} X_L^t = X^t + \vec{b}\,d^t, \\ X_R^t = X^t - \vec{b}\,d^t, \end{cases} \tag{7}$$

where X_t means one beetle position, X_L^t is the left antennae position, X_R^t is the right antennae position, and d^t represents the antennae length in the t-th iteration. The beetle will find the searching behavior based on the detected odor. So, BAS can judge the next beetle position by the strength of the odor. The next beetle position can be updated with the following formula:

$$X^t = X^{t-1} - \vec{b}\,\delta^t \mathrm{sign}\left(f\left(X_L^t\right) - f\left(X_R^t\right)\right), \tag{8}$$

where δ_t means the searching step, sign(.) indicates the sign function, and f(.) is the objective function. The antennae length and the searching step can be expressed as

$$d^t = 0.95d^{t-1} + 0.01, \tag{9}$$

$$\delta^t = 0.95\delta^{t-1}. \tag{10}$$

The iterative process of the beetle antennae search algorithm can be presented as follows:

Step 1: define the maximum iteration $t_{\max}$. Set all BAS initial parameters including the initial step size, the initial antennae length, the population size N, and the searching dimension D. Randomly initialize N beetle positions. Set $t = 0$.

Step 2: update a random vector by equation (6). Update the left-right antennae position by equation (7). Calculate next beetle position by equation (8).

Step 3: update the beetle antennae length by equation (9). Update the beetle searching step by equation (10).

Step 4: compute all function solutions and find the best solution in the current generation. Then, compare the best solution in the current generation with the best solution in the previous generation, and update and record the global optimum solution if there is a better solution.

Step 5: calculate $t = t + 1$. If t is greater than the maximum number of cycles $t_{\max}$, output the current global optimum value. Otherwise, jump to Step 2.

3.2. The Proposed Beetle Antennae Search Algorithm. For basic BAS, the initial sensing length and the initial step size will be selected by human experiences, and the attenuation coefficient is fixed, which can cause that the local searching

process and feasible solutions near the local optimum are not sufficient. Parameters selected by natural selection not only have a strong dependence on design experiences but also have a complicated setting process, time-consuming and laborious. In engineering applications, the parameter selection process must consider environments, errors, disturbances, and other factors, so the parameters got by human experiences are still limited in practical engineering. To solve restriction problems and reduce the probability of being trapped in basic BAS. This paper introduces an enhanced beetle antennae search algorithm with the variable weight method, and the proposed algorithm is called the variable weight beetle antennae search algorithm (VWBAS). VWBAS used the exponential equation in BAS to improve BAS exploration abilities, minimize the searching viciousness, and refrain from falling into the local feasible solution. The variable weight factor r can be expressed as follows:

$$r = e^{-(\mathrm{UB}-\mathrm{LB})\left(t/t_{\max}\right)}, \tag{11}$$

where UB is the upper searching bound and LB is the lower searching bound, and $t_{\max}$ is the maximum iteration. The new step size can be seen by

$$\delta^t_{\mathrm{new}} = \mathrm{wr}|\mathrm{UB} - \mathrm{LB}|, \tag{12}$$

where w is a random factor in the range of [−1, 1].

The new antennae length can be seen by

$$d^t_{\mathrm{new}} = \mathrm{wr}. \tag{13}$$

The new left and right positions can be seen by

$$\begin{cases} X^t_{\mathrm{newL}} = X_{\mathrm{best}} + \overrightarrow{b}\, d^t_{\mathrm{new}}, \\ X^t_{\mathrm{newR}} = X_{\mathrm{best}} - \overrightarrow{b}\, d^t_{\mathrm{new}}. \end{cases} \tag{14}$$

The new next position can be seen by

$$X^t_{\mathrm{new}} = \delta^t_{\mathrm{new}}\, \overrightarrow{b}\, \mathrm{sign}\left(f\left(X^t_{\mathrm{newL}}\right) - f\left(X^t_{\mathrm{newR}}\right)\right). \tag{15}$$

To expand the searching capability, the difference between the upper searching bound and the lower searching bound is set to the searching range. The factor can enhance the searching diversity of feasible solutions for optimization functions. Besides, the proposed algorithm has zero selection factor, which can weaken the blindness and the hysteresis in basic BAS. The VWBAS main step can be summarized in the pseudocode shown in Algorithm 1.

4. Numerical Testing Results and Discussion

4.1. Numerical Testing Parameters. To comprehensively demonstrate the searching accuracy and the iteration speed of the proposed algorithm, sixteen numerical functions listed in Table 1 were calculated in this paper. Calculated numerical functions include ten low-dimension functions and six high-dimension functions. In Table 1, D indicates the searching dimension space, and the aim indicates the ideal value. Low-dimension functions mainly include one-dimension functions and two-dimension functions, which is easy to find the optimal function value. The searching speed and the calculation efficiency will reduce with the searching dimension increasing when algorithms handle high-dimension functions, which enhances the solving of deception. So, low-dimension functions can test algorithm searching speed, and high-dimension functions can test resistance to precocity in algorithms. Compared algorithms include butterfly optimization algorithm (BOA) [38], cuckoo search algorithm (CS) [39], flower pollination algorithm (FPA) [40], simulated annealing (SA) [41], and basic BAS. For BOA, the power exponent was increased from 0.1 to 0.3, factor c was equal to 0.01, and the switch factor p was equal to 0.8. For FPA, parameter p was equal to 0.8, parameter β was equal to 1.5. For FPA, the power exponent was increased from 0.1 to 0.3, factor c was 0.01, and the switch factor p was 0.8. For CS, the parameter pa was equal to 0.25 and the parameter α was equal to 1. For SA, parameter T was equal to 100 and parameter k was equal to 0.95. All algorithm parameters were selected by the original algorithm literature, and all algorithm steps can be found in the original algorithm literature. Each algorithm was independently run ten times in MATLAB (R2014b, the MathWorks, Inc., Natick, MA, USA), the maximum iterations were 500, and the population size was 50.

4.2. Numerical Result Discussion. In Tables 2–4, MIN, MAX, MED, and STD, respectively, represent the minimum function value, the maximum function value, the median function value, and standard deviation. Table 2 shows the two-dimension calculation results. Tables 3 and 4 separately show ten-dimension and twenty-dimension calculation results. From Tables 2–4, the proposed algorithm can find the best aim value for different functions in comparison with the BOA, CS, FPA, and basic BAS. VWBAS can give the minimum value of f_1, f_3, f_4, f_6, and f_7 in Table 2. SD is the arithmetic square root of the variance, which can give the data dispersion. For two groups of data with the same mean, the standard deviation may not be the same. VWBAS has the smallest SD in all algorithms, which displays that the calculated values of VWBAS are closest to the average of all function values. All results in Tables 2–4 can show that the proposed algorithm has a good performance for finding the minimum function value.

4.3. The Wilcoxon Rank-Sum Discussion. The rank-sum test, also known as the sequence sum test, is a nonparametric test. The rank-sum test does not rely on the distribution form, so it can be applied without considering the research object distribution and type [42]. The rank-sum test can be used in the algorithmic analysis to judge whether an algorithm is statistically significant or not. All calculated values will be arranged from small to large, and each calculated value called the rank will be numbered in order. However, the symbol checking only gives the positive and negative signs of the difference and ignores the absolute value of the difference, which will lead to the loss of some experimental information. For deficiencies of the basic rank-sum test, Wilcoxon introduced an enhanced rank-sum test called the Wilcoxon rank-sum test. This method

Input: define all initial parameters. Set searching dimension and population size. Best position X^*. Best function value F. [LB UB]. Set T. $t = 1$.
Output: F.
For 1 ($t = 1 : T$)
  For 2 ($i = 1 : N$)
    Set the random searching direction by equation (6).
    Define the variable weight factor by equation (11).
    Define the new step size by equation (12).
    Define new antennae length by equation (13).
    Calculate new left and right positions by equation (14).
    Calculate the next position of each beetle by equation (15).
    Calculate each function value $f(X^t_{\text{new}})$.
    If $f(X^t_{\text{new}})$ is better than F
      $F = f(X^t_{\text{new}})$
      $X^* = X^t_{\text{new}}$
    End If
  End For 2
End For 1

Algorithm 1: VWBAS.

Table 1: Benchmark functions.

Name	Formulation	D	Scope	Aim
Bartels Conn	$f_1(x) = \lvert x_1^2 + x_2^2 + x_1 x_2 \rvert + \lvert \sin(x_1) \rvert + \lvert \cos(x_2) \rvert$	2	$[-20, 20]$	1
Brent	$f_2(x) = (x_1 + 10)^2 + (x_2 + 10)^2 + e^{-x_1^2 - x_2^2}$	2	$[-20, 20]$	0
Cube	$f_3(x) = 100(x_2 - x_1^3)^2 + (1 - x_1)^2$	2	$[-20, 20]$	0
Freudenstein Roth	$f_4(x) = (x_1 - 13 + ((5 - x_2)x_2 - 2)x_2)^2 + (x_1 - 29 + ((x_2 + 1)x_2 - 14)x_2^2)^2$	2	$[-10, 10]$	0
Himmelblau	$f_5(x) = (x_1^2 + x_2 - 11)^2 + (x_1 + x_2^2 - 7)^2$	2	$[-10, 10]$	0
Leon	$f_6(x) = 100(x_2 - x_1^2)^2 + (1 - x_1)^2$	2	$[-10, 10]$	0
Levy13	$f_7(x) = \sin^2(3\pi x_1) + (x_1 - 1)^2[1 + \sin^2(3\pi x_2)] + (x_2 - 1)^2[1 + \sin^2(2\pi x_2)]$	2	$[-10, 10]$	0
Matyas	$f_8(x) = 0.26(x_1^2 + x_2^2) - 0.48 x_1 x_2$	2	$[-20, 20]$	0
Rotated Ellipse 2	$f_9(x) = x_1^2 - x_1 x_2 + x_2^2$	2	$[-10, 10]$	0
Schaffer N.2	$f_{10}(x) = 0.5 + ((\sin^2(x_1^2 - x_2^2) - 0.5)/([1 + 0.001(x_1^2 + x_2^2)]^2))$	2	$[-20, 20]$	0
ABC	$f_{11}(x) = \sum_{i=1}^{D} \lvert x_i \rvert$	10/20	$[-2, 2]$	0
Ackley	$f_{12}(x) = -20 \exp(-0.2\sqrt{(1/D)\sum_{i=1}^{D} x_i^2}) - \exp((1/D)\sum_{i=1}^{D} \cos(2\pi x_i^2)) + 20 + \exp(1)$	10/20	$[-2, 2]$	0
Girewank	$f_{13}(x) = \sum_{i=1}^{D} (x_i^2/4000) - \prod_{i=1}^{D} \cos(x_i/\sqrt{i}) + 1$	10/20	$[-2, 2]$	0
Levy	$f_{14}(x) = \sin^2(\pi w_1) + \sum_{i=1}^{D-1} (w_i - 1)^2[1 + 10 \sin^2(\pi w_i + 1)] + (w_D - 1)^2[1 + \sin^2(2\pi w_D)]$ $w_i = 1 + ((x_i - 1)/4)$	10/20	$[-2, 2]$	0
Rotated hyperellipsoid	$f_{15}(x) = \sum_{i=1}^{D} \sum_{j}^{i} x_j^2$	10/20	$[-2, 2]$	0
Sum of different powers	$f_{16}(x) = \sum_{i=1}^{D} \lvert x_i \rvert^{i+1}$	10/20	$[-2, 2]$	0

gives not only a different direction but also a different size. This method gives not only a different direction but also a different size. The Wilcoxon rank-sum test can test whether the distribution of the group testing data is different. The Wilcoxon rank-sum test results are called the p value. If the p value is less than 0.05, the value calculated by the algorithm is a significant difference at a level of 0.05. This paper computed the Wilcoxon rank-sum test to show the algorithm significance analysis, and all results were listed in Table 5. Table 5 shows the proposed algorithm results against those of other algorithms at a 0.05 significance level. From Table 5, we can find that all results were less than 0.05, which displays that the proposed algorithm can give large searching efficiency and avoid falling into a local optimal solution.

4.4. Iteration Discussion. To describe the searching ability and the iteration speed of the proposed algorithm more intuitively, this paper used the y-logarithmic coordinate system. Logarithmic coordinates refer to the point position corresponding to the logarithm image in the two-

Table 2: Two-dimension benchmark function results.

Function	Results	Algorithm					
		VWBAS	BAS	BOA	CS	FPA	SA
f_1	MIN	1	1.0000	1.0008	1.0034	1.0043	1.0012
	MAX	1	1.0149	1.0147	1.2728	1.0185	1.0101
	MED	1	1.0019	1.0105	1.0754	1.0088	1.0042
	STD	0	0.0045	0.0046	0.0795	0.0048	0.0033
f_2	MIN	$1.3839E-87$	$1.4119E-24$	0.0097	0.0063	$1.2854E-05$	$1.3461E-04$
	MAX	$1.3839E-87$	$4.9731E-23$	4.1302	0.0783	0.0011	0.0018
	MED	$1.3839E-87$	$9.4007E-24$	0.5519	0.0167	$2.6758E-04$	$7.2868E-04$
	STD	$2.3532E-103$	$1.4724E-23$	1.3312	0.0287	$4.7333E-04$	$5.0677E-04$
f_3	MIN	0	0.0186	$4.3768E-05$	0.0021	0.0017	$5.0843E-05$
	MAX	0	0.1551	0.0227	0.8989	0.1691	0.0593
	MED	0	0.0884	0.0017	0.3315	0.0099	0.0038
	STD	0	0.0383	0.0081	0.3037	0.0541	0.0179
f_4	MIN	0	$9.3792E-06$	0.0503	0.0099	$5.0293E-04$	$3.6766E-04$
	MAX	0	1.5265	4.6892	2.1039	0.0395	0.0641
	MED	0	0.0103	0.8393	0.3211	0.0097	0.0176
	STD	0	0.4771	1.5894	0.6029	0.0147	0.0204
f_5	MIN	0	$1.4279E-07$	0.0016	0.0036	$7.2210E-05$	$1.1476E-04$
	MAX	$7.8886E-31$	$5.5746E-05$	0.8472	0.2136	0.0280	0.0055
	MED	$7.8886E-31$	$3.5741E-06$	0.0507	0.0582	0.0058	0.0010
	STD	$4.0737E-31$	$1.8134E-05$	0.2590	0.0676	0.0085	0.0015
f_6	MIN	0	$7.8128E-05$	$5.2822E-05$	0.0077	$6.8104E-04$	$2.0819E-05$
	MAX	0	0.0789	0.0187	0.2464	0.0077	0.0034
	MED	0	0.0078	0.0030	0.0714	0.0025	$9.1410E-04$
	STD	0	0.0237	0.0065	0.0814	0.0025	0.0011
f_7	MIN	$1.3498E-31$	$3.7740E-05$	$4.0847E-04$	0.0063	$1.3159E-04$	$8.9750E-05$
	MAX	$1.3498E-31$	0.0284	0.1602	0.3104	0.0100	0.0010
	MED	$1.3498E-31$	0.0020	0.0021	0.0676	0.0017	$3.4180E-04$
	STD	0	0.0085	0.0521	0.1044	0.0036	$3.2428E-04$
f_8	MIN	$4.6959E-71$	$1.4201E-26$	0.0047	$4.5054E-04$	$1.0869E-04$	$3.7807E-07$
	MAX	$1.4549E-69$	$2.3812E-25$	0.0177	0.0140	$9.1187E-04$	$1.6527E-05$
	MED	$2.9429E-70$	$4.9884E-26$	0.0115	0.0012	$2.5820E-04$	$5.8093E-06$
	STD	$4.7398E-70$	$6.4679E-26$	0.0043	0.0042	$3.2265E-04$	$5.5580E-06$
f_9	MIN	$1.1076E-37$	$3.1093E-26$	0.0117	$8.8083E-05$	$5.1297E-05$	$2.4619E-06$
	MAX	$1.1221E-35$	$9.6231E-25$	0.0229	0.0210	0.0015	$1.5049E-04$
	MED	$2.8907E-36$	$3.0909E-25$	0.0166	0.0036	$2.2176E-04$	$2.0898E-05$
	STD	$3.6248E-36$	$2.8201E-25$	0.0041	0.0075	$4.2105E-04$	$6.2283E-05$
f_{10}	MIN	0	0	$1.6142E-04$	$4.3043E-13$	$4.3582E-11$	$2.0464E-12$
	MAX	0	0.2911	0.0016	$1.0831E-05$	$3.7154E-08$	$3.7675E-06$
	MED	0	0.0446	$6.7551E-04$	$1.6984E-06$	$7.6009E-09$	$1.1603E-09$
	STD	0	0.1133	$4.0116E-04$	$3.6951E-06$	$1.1715E-08$	$1.5683E-06$

dimensional rectangular coordinate system, and the curve maximum variation range can be extended to make the figure outline clear in the logarithmic coordinate system. So, this paper used the semilogarithmic coordinate to show function values. Iterations are repeating feedback actions, and each iteration result will be the initial value for the next iteration. Figures 3 and 4 show the different dimension average iteration curves of all algorithms under 10 independent runs. It must be mentioned here that all iteration curves are average convergence curves. In iteration figures, the proposed algorithm owns the largest iteration speed and the best searching accuracy in all iteration curves, which displays that VWBAS can improve the feasible solution diversity. VWBAS owns the good performance to jump out of the local optimum in high-dimension iteration figures and low-dimensional iteration figures. Iteration results determine that the proposed algorithm can not only give an outstanding balance but also can jump from local optimal solution in the searching field.

4.5. Box-Plot Chart Discussion. The box-plot chart is a statistical chart, which can not only exhibit a set of dispersed data but also be applied in several experiments to analyze the data symmetry. There are five indexes in a box-plot chart, including the maximum value, the minimum value, the median, the upper quartile, and the lower quartile. Figure 5 gives two-dimension box-plot charts. Figure 6 separately shows ten-dimension and twenty-dimension box-plot charts. Figures 5 and 6 clearly emphasize that VWBAS box-plot charts own the

Table 3: Ten-dimension benchmark function results.

Function	Results	Algorithm					
		VWBAS	BAS	BOA	CS	FPA	SA
$f_{11(D=10)}$	MIN	$5.1495E-04$	0.7805	0.1231	3.1714	1.9561	1.2126
	MAX	0.0012	2.6108	0.1720	4.9107	3.7099	2.0280
	MED	$8.0524E-04$	1.4344	0.1629	3.9385	2.7443	1.6677
	STD	$2.3991E-04$	0.5128	0.0141	0.5877	0.5360	0.2645
$f_{12(D=10)}$	MIN	$2.8628E-04$	1.3136	0.1053	2.6644	2.1694	1.0628
	MAX	$4.8183E-04$	2.3147	0.1166	3.7868	3.0995	2.4624
	MED	$3.6869E-04$	1.8689	0.1115	3.2280	2.5199	2.0251
	STD	$5.5464E-05$	0.2944	0.0038	0.3359	0.3655	0.3722
$f_{13(D=10)}$	MIN	$6.2884E-09$	0.0299	0.0083	0.1864	0.1119	0.0339
	MAX	$1.5772E-08$	0.0749	0.0107	0.3184	0.2127	0.0661
	MED	$1.0151E-08$	0.0477	0.0098	0.2484	0.1291	0.0513
	STD	$2.9684E-09$	0.0136	$8.1062E-04$	0.0458	0.0387	0.0114
$f_{14(D=10)}$	MIN	$2.9037E-08$	0.0019	0.4067	0.3607	0.2489	0.1836
	MAX	$1.4939E-07$	0.1533	0.9528	0.9065	0.4316	0.2700
	MED	$5.9598E-08$	0.1075	0.7163	0.6461	0.3185	0.2172
	STD	$4.1907E-08$	0.0402	0.1771	0.1823	0.0553	0.0289
$f_{15(D=10)}$	MIN	$4.4689E-07$	0.4125	0.0314	5.6038	2.8744	1.6929
	MAX	$1.1385E-06$	2.4806	0.0394	17.3462	10.5713	3.0986
	MED	$7.4017E-07$	1.2556	0.0361	10.6256	5.3429	1.9800
	STD	$2.4581E-07$	0.6993	0.0024	3.6134	2.7715	0.4384
$f_{16(D=10)}$	MIN	$1.4351E-09$	$7.9685E-04$	$9.9636E-04$	0.3012	0.1611	0.0083
	MAX	$7.1362E-09$	0.0498	0.0023	2.7134	0.5775	0.0314
	MED	$3.4424E-09$	0.0088	0.0016	1.4869	0.2871	0.0211
	STD	$2.2149E-09$	0.0195	$4.3366E-04$	0.7201	0.1471	0.0085

Table 4: Twenty-dimension benchmark function results.

Function	Results	Algorithm					
		VWBAS	BAS	BOA	CS	FPA	SA
$f_{11(D=20)}$	MIN	0.0019	6.1884	0.2223	8.3316	10.0417	6.0262
	MAX	0.0027	7.7539	0.2537	11.9289	11.7899	7.0740
	MED	0.0019	7.0443	0.2381	11.4304	10.5701	6.4881
	STD	$3.1515E-04$	0.5284	0.0092	1.2513	0.6601	0.3335
$f_{12(D=20)}$	MIN	$3.0761E-04$	2.9730	0.1131	4.1466	3.6298	2.8304
	MAX	$4.3775E-04$	3.6085	0.1219	4.5172	4.2881	3.3600
	MED	$4.0137E-04$	3.4027	0.1165	4.3406	3.9256	3.1457
	STD	$4.6638E-05$	0.2033	0.0029	0.1139	0.2245	0.1626
$f_{13(D=20)}$	MIN	$1.1814E-08$	0.2149	0.0104	0.4471	0.4004	0.1572
	MAX	$5.1979E-08$	0.3223	0.0131	0.5749	0.4872	0.2622
	MED	$2.0117E-08$	0.2499	0.0120	0.5070	0.4393	0.1996
	STD	$1.1538E-08$	0.0388	$8.1352E-04$	0.0393	0.0359	0.0312
$f_{14(D=20)}$	MIN	$1.5689E-07$	0.7937	1.6745	2.0988	1.9808	0.7202
	MAX	0.2686	1.2500	2.0793	3.7024	2.5881	1.0460
	MED	$3.6230E-07$	0.9687	1.8457	2.9394	2.1810	0.8776
	STD	0.0870	0.1385	0.1434	0.4927	0.2023	0.0837
$f_{15(D=20)}$	MIN	$2.9463E-06$	32.1296	0.0498	68.3577	46.2623	23.2547
	MAX	$1.6725E-05$	60.0866	0.0558	126.4884	87.1203	32.9357
	MED	$5.2569E-06$	44.1930	0.0536	88.8603	67.2462	29.4419
	STD	$3.8988E-06$	8.8406	0.0019	17.6243	12.1793	3.4255
$f_{16(D=20)}$	MIN	$1.5402E-08$	1.9921	$6.6078E-04$	$1.2309E+06$	$3.0583E+05$	0.0962
	MAX	$4.2269E-08$	8.2239	0.0028	$6.0122E+08$	$1.0879E+07$	1.1136
	MED	$2.6599E-08$	3.9392	0.0015	$3.7144E+07$	$2.0862E+06$	0.2017
	STD	$8.6398E-09$	2.0329	$6.2304E-04$	$1.9657E+08$	$3.2839E+06$	0.3244

Table 5: The Wilcoxon rank-sum results.

Function	Algorithm				
	BAS	BOA	CS	FPA	SA
f_1	$6.39E-05$	$6.39E-05$	$6.39E-05$	$6.20E-05$	$6.39E-05$
f_2	$6.39E-05$	$6.39E-05$	$6.39E-05$	$6.25E-05$	$6.39E-05$
f_3	$6.39E-05$	$6.39E-05$	$6.39E-05$	$6.20E-05$	$6.39E-05$
f_4	$6.39E-05$	$6.39E-05$	$6.39E-05$	$6.29E-05$	$6.39E-05$
f_5	$1.41E-04$	$1.41E-04$	$1.41E-04$	$1.38E-04$	$1.41E-04$
f_6	$6.39E-05$	$6.39E-05$	$6.39E-05$	$6.25E-05$	$6.39E-05$
f_7	$6.39E-05$	$6.39E-05$	$6.39E-05$	$6.25E-05$	$6.39E-05$
f_8	$1.83E-04$	$1.83E-04$	$1.83E-04$	$1.81E-04$	$1.83E-04$
f_9	$1.83E-04$	$1.83E-04$	$1.83E-04$	$1.80E-04$	$1.83E-04$
f_{10}	$7.51E-04$	$6.39E-05$	$6.39E-05$	$6.25E-05$	$6.39E-05$
$f_{11(D=10)}$	$1.83E-04$	$1.83E-04$	$1.83E-04$	$1.80E-04$	$1.83E-04$
$f_{12(D=10)}$	$1.83E-04$	$1.83E-04$	$1.83E-04$	$1.80E-04$	$1.83E-04$
$f_{13(D=10)}$	$1.83E-04$	$1.83E-04$	$1.83E-04$	$1.79E-04$	$1.83E-04$
$f_{14(D=10)}$	$1.83E-04$	$1.83E-04$	$1.83E-04$	$1.79E-04$	$1.83E-04$
$f_{15(D=10)}$	$1.83E-04$	$1.83E-04$	$1.83E-04$	$1.78E-04$	$1.83E-04$
$f_{16(D=10)}$	$1.83E-04$	$1.83E-04$	$1.83E-04$	$1.80E-04$	$1.83E-04$
$f_{11(D=20)}$	$1.83E-04$	$1.83E-04$	$1.83E-04$	$1.81E-04$	$1.83E-04$
$f_{12(D=20)}$	$1.83E-04$	$1.83E-04$	$1.83E-04$	$1.80E-04$	$1.83E-04$
$f_{13(D=20)}$	$1.83E-04$	$1.83E-04$	$1.83E-04$	$1.79E-04$	$1.83E-04$
$f_{14(D=20)}$	$1.83E-04$	$1.83E-04$	$1.83E-04$	$1.81E-04$	$1.83E-04$
$f_{15(D=20)}$	$1.83E-04$	$1.83E-04$	$1.83E-04$	$1.79E-04$	$1.83E-04$
$f_{16(D=20)}$	$1.83E-04$	$1.83E-04$	$1.83E-04$	$1.80E-04$	$1.83E-04$

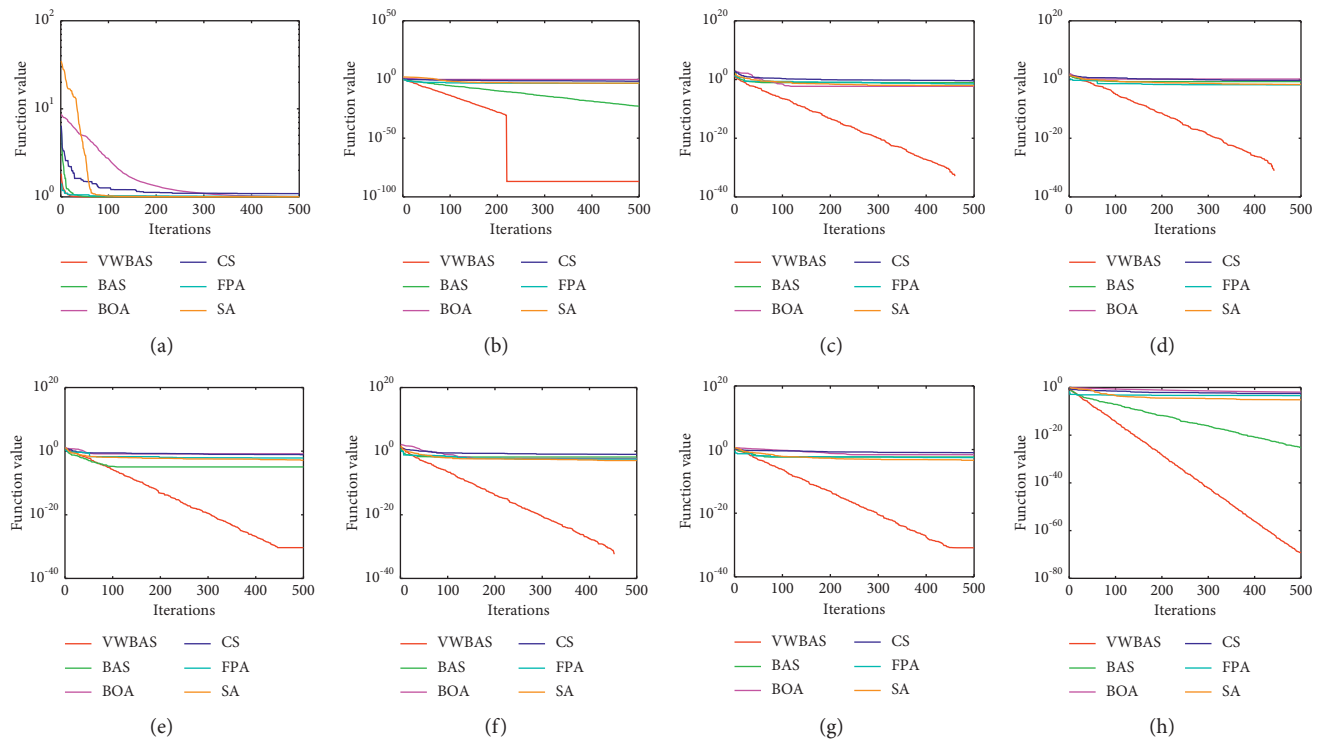

Figure 3: Continued.

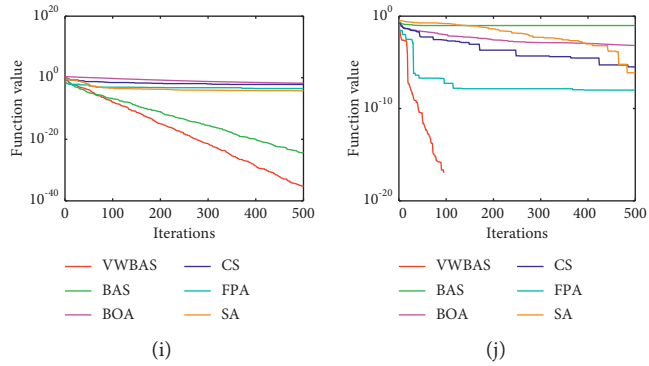

Figure 3: Average iterative curves of two-dimension functions 1–10: (a) f_1. (b) f_2. (c) f_3. (d) f_4. (e) f_5. (f) f_6. (g) f_7. (h) f_8. (i) f_9. (j) f_{10}.

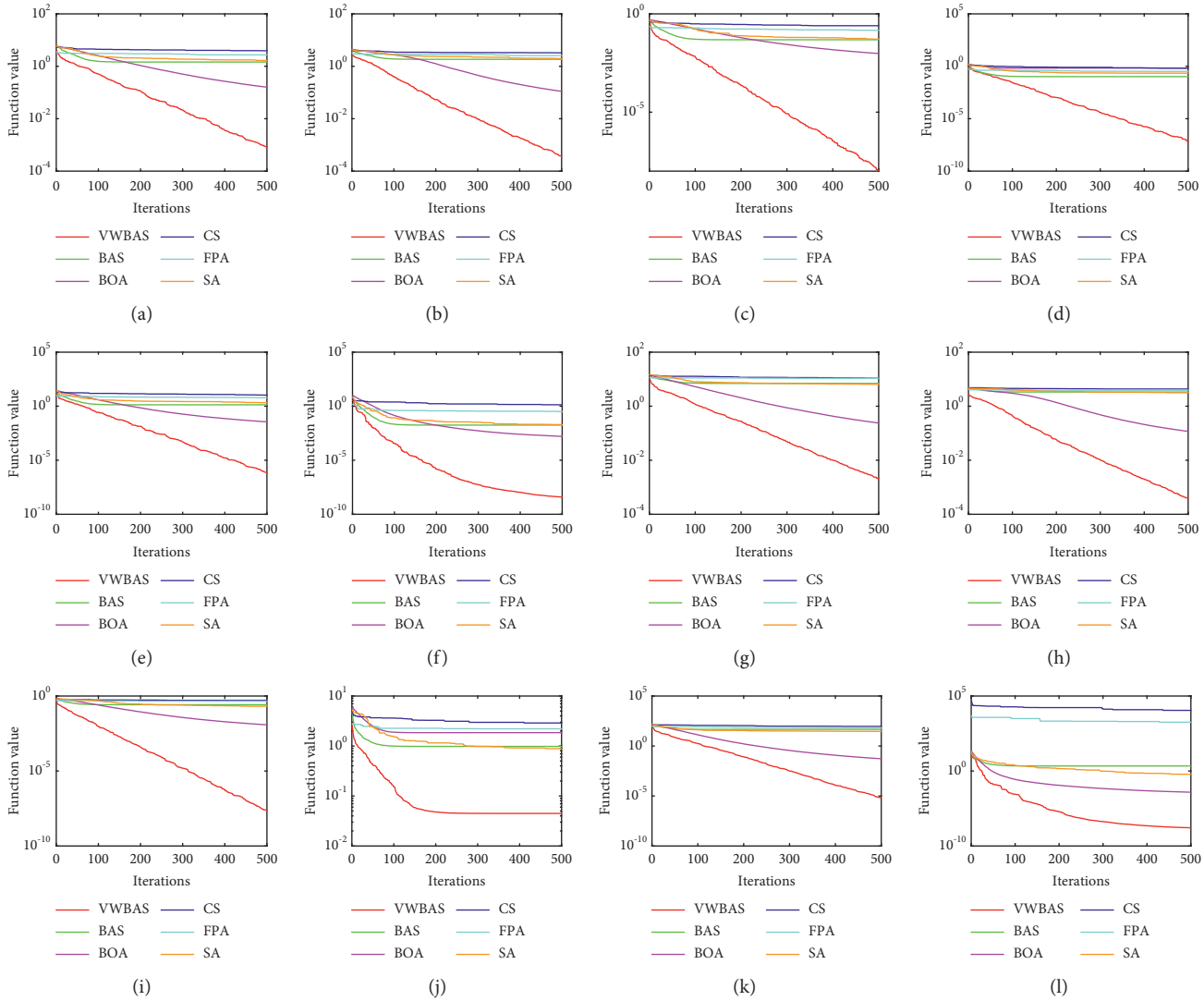

Figure 4: Average iterative curves of high-dimension functions 11–16: (a) $f_{11(D=10)}$. (b) $f_{12(D=10)}$. (c) $f_{13(D=10)}$. (d) $f_{14(D=10)}$. (e) $f_{15(D=10)}$. (f) $f_{16(D=10)}$. (g) $f_{11(D=20)}$. (h) $f_{12(D=20)}$. (i) $f_{13(D=20)}$. (j) $f_{14(D=20)}$. (k) $f_{15(D=20)}$. (l) $f_{16(D=20)}$.

smallest form and the fewest outliers, which shows that the proposed algorithm can give a strong searching ability and the approaching efficiency. Compared with different algorithms, the main reason for the proposed algorithm having the best searching ability is that VWBAS has a balance and exponential explosion method in variable weight mechanism. All

box-plots can determine that VWBAS has statistically significant and does not happen by accident.

4.6. Searching Path Discussion. To inspect the effectiveness of searching orientation ability, this paper carries on a searching path comparative experiment. Figure 7 gives the contour plot of each function, the optimal BAS searching path, and the optimal VWBAS searching path of low-dimension functions. From Figure 7, we can see that VWBAS searching paths are markedly shorter than BAS searching paths. BAS searching paths have many long, invalid, and repeat distances, and it can be seen that the BAS method searches have a longer path because of the unbalance between exploration and repulsive effect, which is more dangerous in practical applications. Through different experiment analyses, we found that the searching direction of the proposed algorithm has strong random and efficient computing ability. Because the searching path after the left-right exploration is almost the same, a lot of calculated time is weakened. Therefore, for the proposed algorithm, all box-plots can determine that VWBAS is statistically significant and has merit in terms of exploration, and it does not happen by accident. A small number of iterations can give a better path, which is profitable for path planning in the nonconvex bounded constraint.

5. The PID Tuning Strategy

5.1. PID Controller. A PID controller has three parameters including the proportional parameter K_p, the differential parameter K_d, and the integral parameter K_i. The parameter K_p can reflect the deviation quickly and can reduce the deviation, K_d can reflect the changing trend of deviation signals, and K_i is mainly used to eliminate the static error and improve the system accuracy. Selecting appropriate PID parameters makes systems have a perfect response speed and good performance. There are two models in the current PID controller, including the continuous form and the discrete form.

The PID continuous form can be written as

$$u(t) = K_p e(t) + K_i \int_0^t e(t)\mathrm{d}t + K_d \frac{\mathrm{d}e(t)}{\mathrm{d}t}, \tag{16}$$

where K_p is the proportional parameter, K_i is the integral parameter, K_d is the derivative parameter, $u(t)$ is the PID control signal, and $e(t)$ is the system error signal.

The PID discrete form can be written as

$$u(k) = K_p e(k) + K_i T \sum_{k=0}^{a} e(k) + \frac{K_d}{T}\left(e(k) - e(k-1)\right), \tag{17}$$

where k is the once sampling number, T is the sampling period, and a is the total sampling number.

5.2. Evaluation Function. Before the PID tuning process, a reasonable system evaluation function should be selected. Evaluation functions can be divided into two types including the single objective function and the mixed objective functions. Before the PID tuning process, a reasonable system evaluation function should be selected. Evaluation functions can be divided into two types including the single evaluation function and the mixed objective functions. The single-objective function includes the IAE (integration absolute value error) and the ISE (integration square value error). The mixed evaluation function includes the ITAE (integration time absolute value error), the MSE (mean square value error), and the ITSE (integration time square value error). The IAE only considers a single factor and pays attention to the absolute error, so it is often used in a digital simulation system. And it is difficult to get the absolute error value in the real state of hydraulic systems. Because the square of large error is much larger in the ISE, the large error will be punished more than the small error. Although selecting ISE as the evaluation function will quickly weaken the large error, the system will tolerate small errors for a long time. The MSE can weaken the disadvantage of ISE by calculating the average value of the ISE, but the system has to run for a long time. A time multiplication is added into the ITAE to punish and weigh the long-term error. The ITSE has extra time to punish errors in ITAE. To obtain a good tuning result, this paper selects a hybrid index with the linear weighted method ITSE:

$$\mathrm{ITSE} = \int_0^t te^2(t)\mathrm{d}t, \tag{18}$$

where $e(t)$ is the system error. ITSE can not only avoid a too large signal value that can be beyond the amplitude of the PID controller but also avoid the excessive error rate which can cause the sensor delay in the control system.

5.3. Tuning Method Design. PID controller parameters determine the control performance and the control accuracy. So, one of the core problems in the design and application of PID controller is the parameter tuning method. To enhance the control performance of hydraulic systems and the effectiveness and practicability of PID controllers, this paper will design a PID tuning method based on VWBAS to find reasonable PID controller parameters for better driving hydraulic systems. The working principle of the proposed tuning method is to transform the PID parameter selection problem into the algorithm-solving three-dimensional optimization problem. PID controller parameters can be regarded as the individual position in the three-dimensional space. When the controlled system starts to run, the VWBAS automatically calculates the selected system evaluation function value, and the solution of the minimum system evaluation function value is regarded as the best PID controller parameter result. The flowchart of the proposed PID tuning method is shown in Figure 8.

The specific search steps in flowchart can be described as follows:

Step 1: initialization

Initialize VWBAS parameters. The dimension of searching space is defined as the matrix $[K_p\, K_i\, K_d]$. In

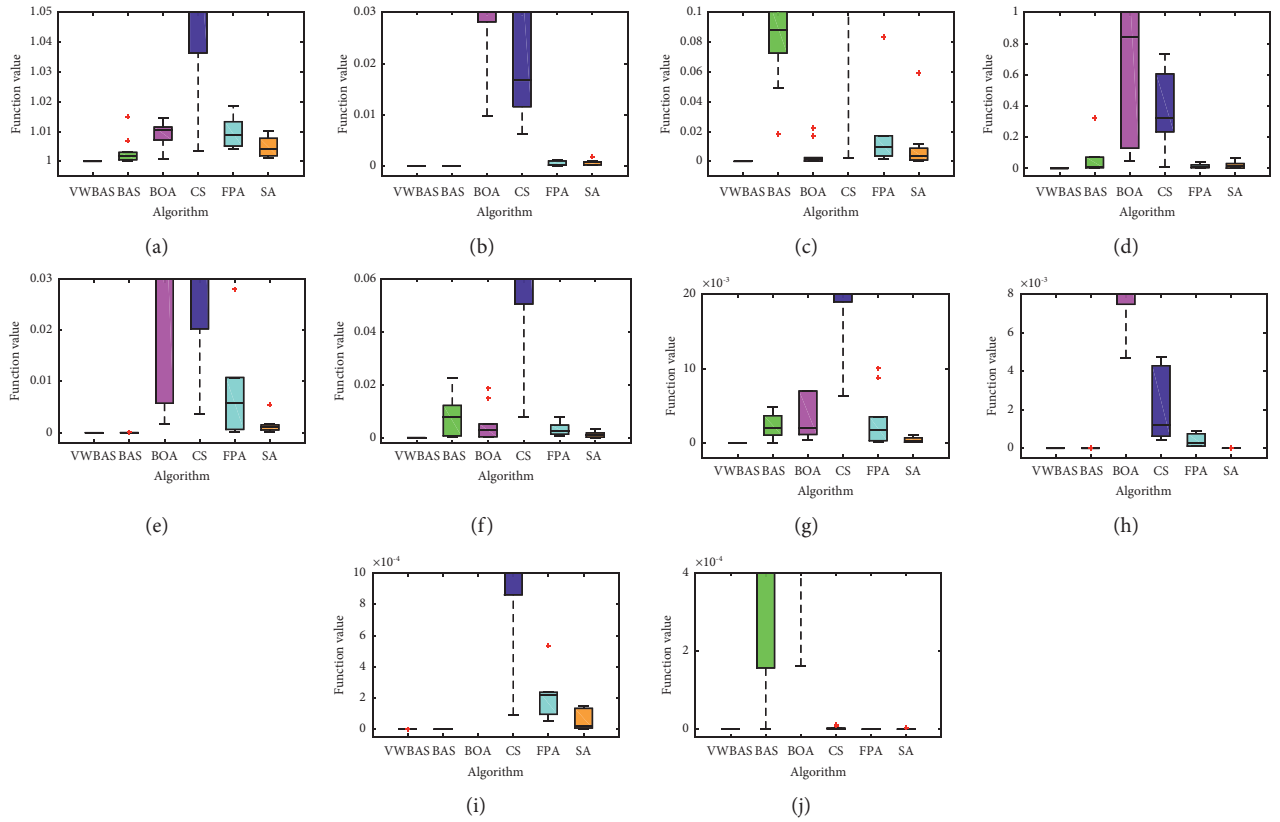

Figure 5: Box-plot charts of two-dimension functions: (a) f_1. (b) f_2. (c) f_3. (d) f_4. (e) f_5. (f) f_6. (g) f_7. (h) f_8. (i) f_9. (j) f_{10}.

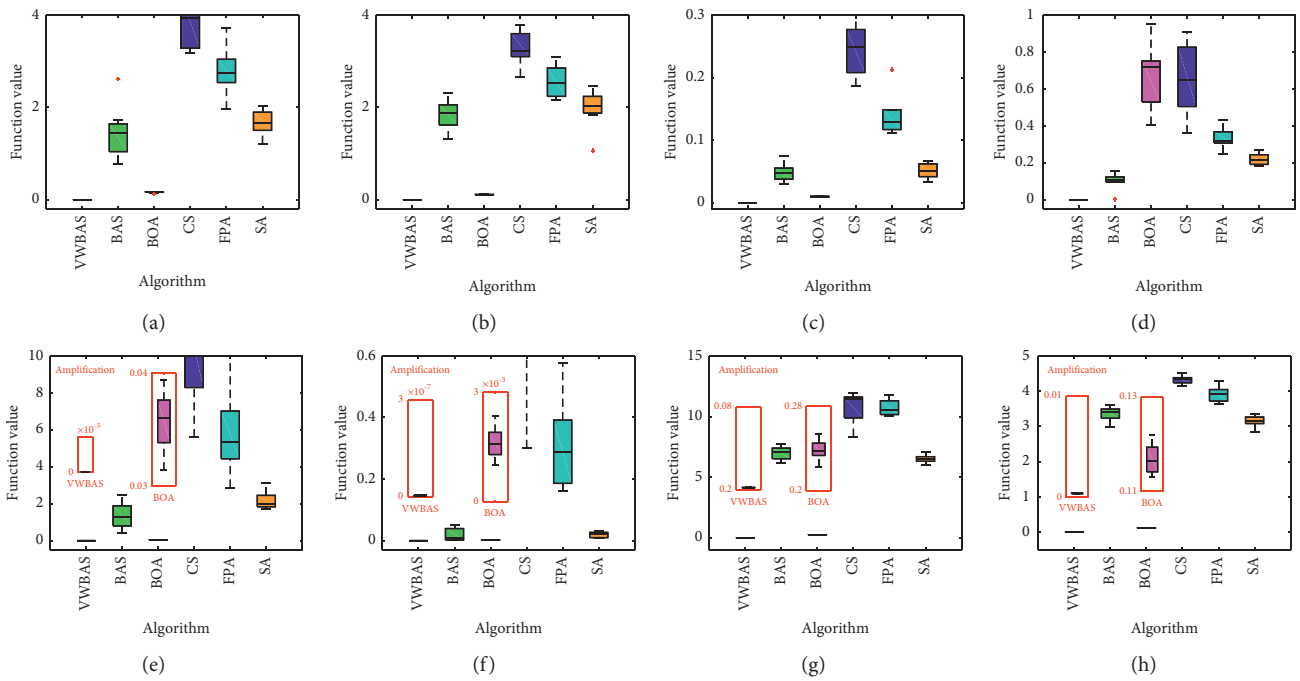

Figure 6: Continued.

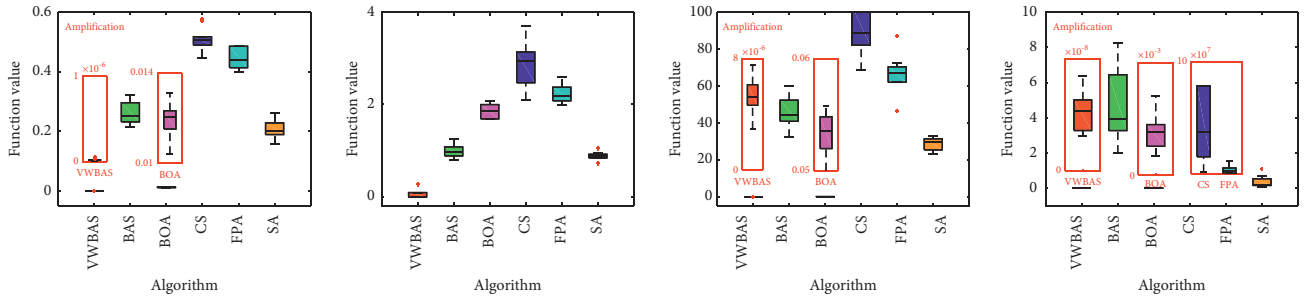

Figure 6: Box-plot charts of high-dimension function: (a) $f_{11(D=10)}$. (b) $f_{12(D=10)}$. (c) $f_{13(D=10)}$. (d) $f_{14(D=10)}$. (e) $f_{15(D=10)}$. (f) $f_{16(D=10)}$. (g) $f_{11(D=20)}$. (h) $f_{12(D=20)}$. (i) $f_{13(D=20)}$. (j) $f_{14(D=20)}$. (k) $f_{15(D=20)}$. (l) $f_{16(D=20)}$.

the three-dimensional searching space, algorithm population positions are randomly generated. Define the maximum number of search iterations K and set $k = 1$.

Step 2: variable weight beetle antennae search algorithm

In the first step, the yellow population can be seen as the old position in Figure 8. In the second step, run the algorithm. In the third step, the pink population can be seen as the new position in Figure 8. All positions can be seen as PID controller parameters.

Step 3: control system

Input the control signal to run the control system. Red population positions in Figure 8 will be input into the PID controller as three parameters, and the control system is run to calculate the ITSE value. In Figure 8, step represents the unit step signal.

Step 4: evaluate function

Compare all ITSE values and find out the minimum ITSE value in the current iteration. Compare the minimum ITSE value in the current iteration with the minimum ITSE value in the last iteration. The position of the global minimum ITSE value is defined as the global optimal solution. The global minimum ITSE value is selected, and the global optimal solution is updated.

Step 5: determine the iteration stop

Judge whether the iteration numbers meet the iteration termination condition $K = k$. If k is equal to K, stop the iteration. The global optimal solution is taken as the final PID parameter. If K is not equal to k, calculate $k = k + 1$ and return to Step 2.

6. Hydraulic System Result and Discussion

6.1. System Parameters. To show the performance of the proposed method, this paper carried out different PID controllers in MATLAB. The analysis object is the semi-physical simulation platform shown in Figure 9. The platform includes the signal acquisition card, the hydraulic oil source, and other hydraulic systems. Hydraulic systems include the actuator cylinder, the force and position sensor, a sliding guide rail, a piston rod, different loading, the hydraulic oil, and so on. This paper compared VWBAS with different algorithms in the above analysis, so testing methods in this paper selected genetic algorithm (GA) [43], particle swarm optimization (PSO) [44], and the Z-N tuning method. For the GA, the crossover probability P_{cross} is equal to 0.8, and the mutation probability P_m is equal to 0.1. For the PSO, parameters were set as learning factors are equal to 1 and the inertia weight is equal to 1. All initial algorithm parameters were chosen by the relevant algorithm literature. The range of PID parameters was generated in [0, 10000]. Set maximum iterations 1000. Set population size 50. Each algorithm was implemented in MATLAB (R2014b, The MathWorks, Inc., Natick, MA, USA). All algorithms were conducted on a laptop with Intel (R) Core (TM) i5-4210U CPU, 2.30 GHz, 4 GB RAM. All data and figures were analyzed in similar MATLAB software.

6.2. Time Response Analysis. Under the action of input signals, the changed process of the system output with time is called the system time response. The time response of an actual system usually consists of two parts: the transient response and the steady-state response. Transient response, which is also known as the dynamic response, refers to the system response action from the zero states to the stable state under a certain action. The transient response reflects the stability and the rapidity of the control system. The steady-state response, which reflects the system accuracy, is the system output state when the running time approaches infinity. So, the dynamic performance of the control system can be evaluated by the system time response of the system. The time response depends not only on the system characteristic but also on the output signal form. The time response performance index is based on the system time-varying process under the unit step signal, mainly includes the maximum overshoot M_p, the delay time t_d, the adjustment time t_s, and the steady-state error e_{ss}. The difference value between the maximum peak value and the steady-state value is called the maximum overshoot. That the running time of the response curve reaches the steady-state value from the original working state is defined as the delay time. The upper and lower bounds of the allowable error range are taken as ±5% or 2% under the steady-state of the response

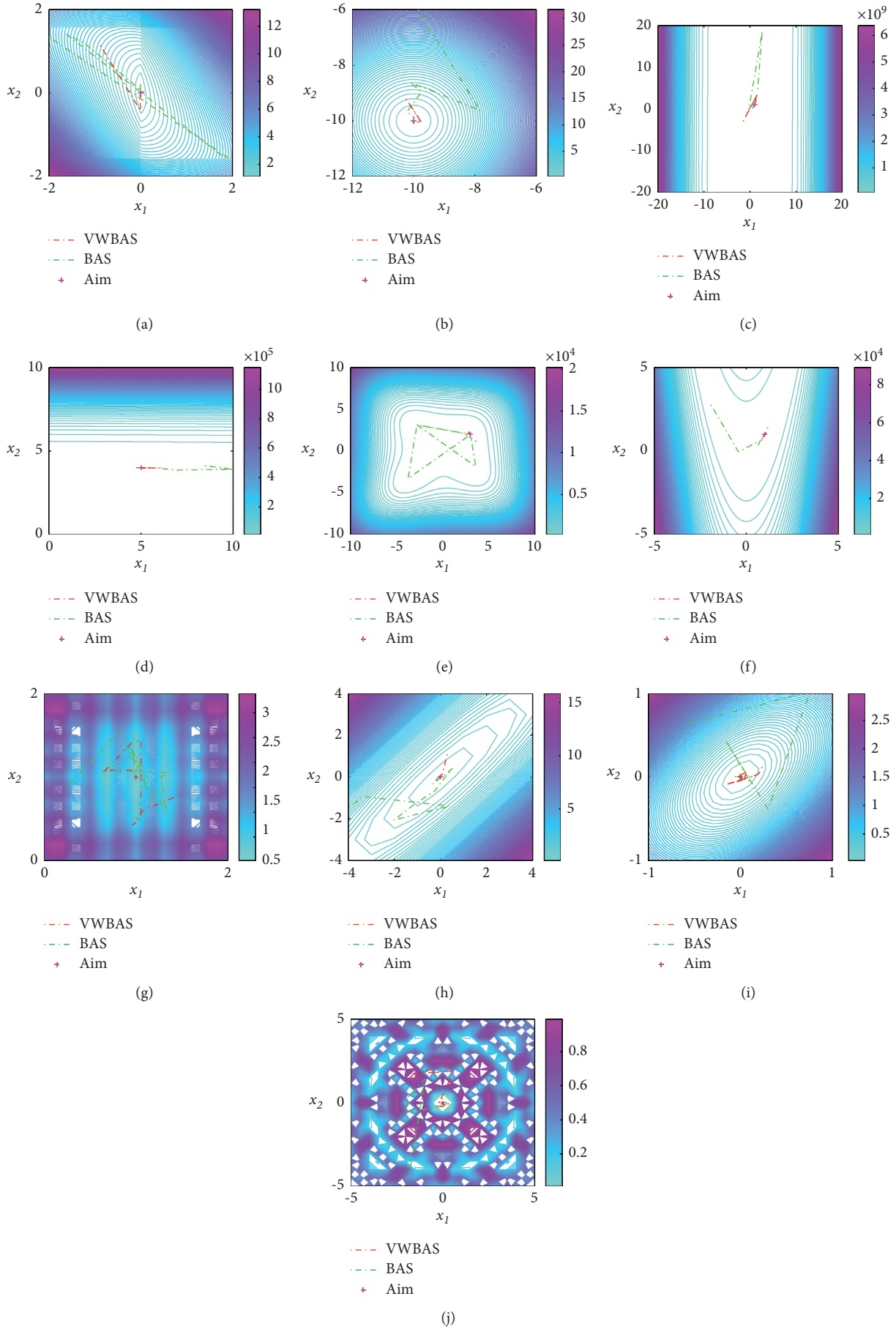

Figure 7: Comparison of searching paths: (a) f_1. (b) f_2. (c) f_3. (d) f_4. (e) f_5. (f) f_6. (g) f_7. (h) f_8. (i) f_9. (j) f_{10}.

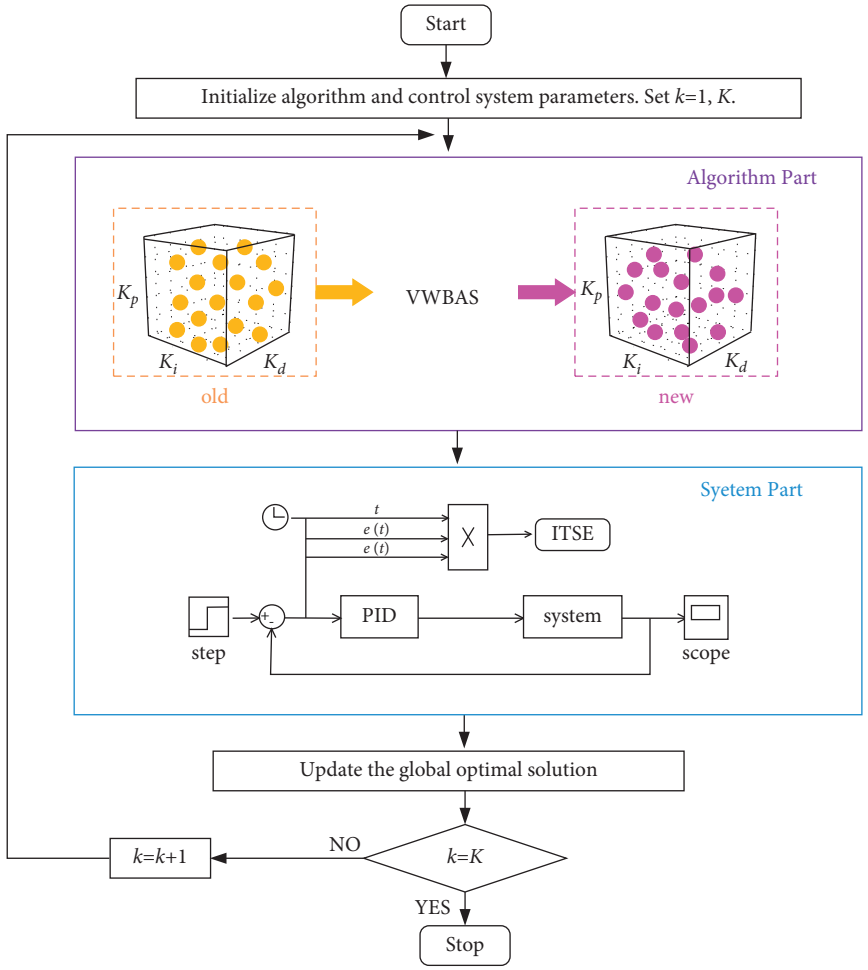

Figure 8: The flowchart of the proposed PID tuning method.

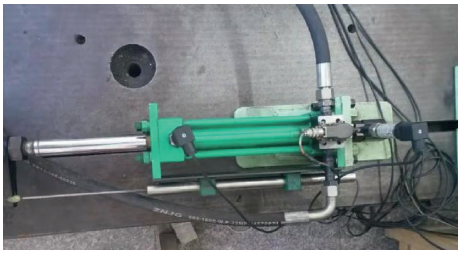

Figure 9: The analysis object.

curve, and that the running time can remain this error range is called the adjustment time. After the system reaches the steady-state, the difference between the steady-state value and the ideal value is called the steady-state error. Table 6 displays ITSE values and indices of the temporal response. The VWBAS tuning method has the lowest ITSE and the smallest M_p, t_s, and e_{ss}. Because ZN is an artificial experience method, ZN does not have ITSE. Although the delay time of the VWBAS-PID is larger than that of the ZN-PID, ZN-PID has the largest M_p, and the error precision is 0.001, which shows that the proposed control method has superior performance. The system time response analysis shows that the proposed method can make the controlled system have a good tracking performance and a fast response speed.

The three-dimension response curve and the two-dimension response curve are shown in Figure 10. The ZN-PID has the maximum overshoot, appears the signal chattering phenomenon. PSO-PID has a too large running time and some extent overshoot, which can cause system vibration and shock, and PSO-PID has some extent overshoot. VWBAS-PID can arrive at the steady-state with the smallest overshoot. The system drove by the VWBAS-PID

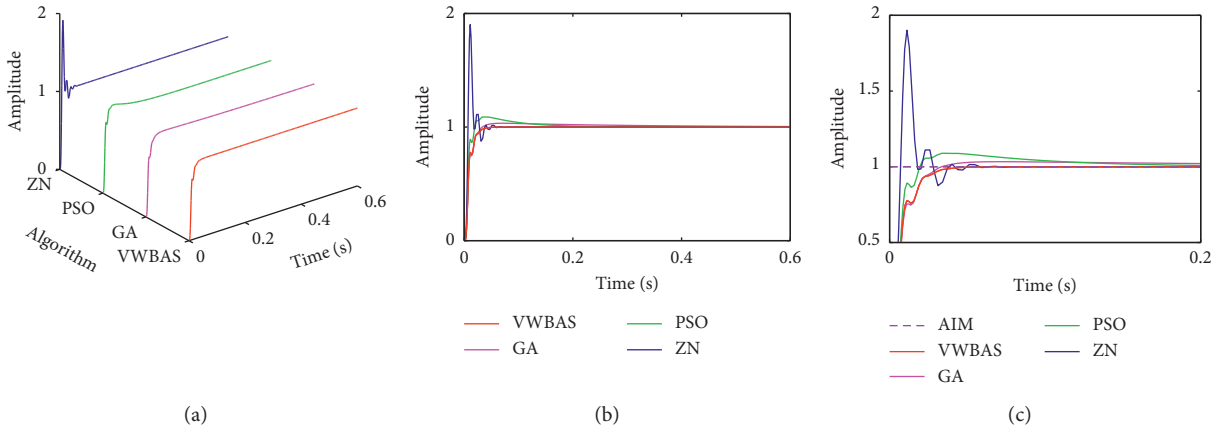

(a) (b) (c)

Figure 10: The step response curves: (a) three-dimension curve; (b) two-dimension curve; (c) local amplification.

Table 6: PID parameters and time response characteristic.

Parameters	Algorithm			
	VWBAS	GA	PSO	ZN
K_p	21.1720	19.5858	23.4461	34.0202
K_i	0.0005	72.1146	311.9005	5376.8467
K_d	0	0.0082	0	0.0517
ITSE	$2.7495E-05$	$4.2524E-05$	$4.6351E-05$	NO
M_p	$5.9886E-04$	0.0335	0.0893	0.9018
t_d	0.0075	0.0084	0.0075	0.0058
t_s	0.0241	0.0243	0.0834	0.0341
e_{ss}	$4.2652E-06$	$9.2185E-06$	$1.0820E-05$	$4.8367E-05$

can maintain good accuracy and safety, demonstrating large serviceability, applicability, and stability. The response curve confirms that the proposed method can quickly track the steady-state in the running stage.

6.3. Frequency Characteristic Analysis. The frequency characteristic analysis is to study the system steady-state response under different sinusoidal signals. In the mechanical engineering field, there are many problems to study the system response characteristic and process under different frequency signals. The frequency characteristic reflects the system self-excited vibration, resonance characteristics, mechanical impedance, dynamic stiffness, and antivibration stability. The machining accuracy, the surface quality, and the self-excited vibration are closely related to the system frequency characteristic in the machining process. Therefore, the frequency characteristic is very important for the analysis and design of mechanical systems. For an ideal system, when a sinusoidal signal is an input, the system output response is still the sinusoidal signal having the same frequency after a long enough time. To further show the frequency characteristic of the system droved by the proposed method, different four sinusoidal signals were input. For different sinusoidal signals, the angular velocities were, respectively, set as 15 and 25, the initial phase was zero, and the amplitude was set to 40 and 80. The response results and the local amplification are presented in Figures 11–14. As we can see in all figures, except for the VWBAS-PID, the other three PID controllers have amplitude outstripping phenomena under different frequency response curves. The system drove by the PSO-PID owns the largest amplitude difference value between the response amplitude and the ideal amplitude. The system controlled by the VWBAS-PID owns the smallest amplitude difference value between the response amplitude and the ideal amplitude, and response curves of the VWBAS-PID controller are closest to the ideal amplitude. Sinusoidal response curves display that the proposed controller can enhance the control accuracy and robustness and owns a favorable ability to return its original equilibrium or give a new equilibrium. Therefore, we can analyze that the proposed method controller has the reinforced ability, the antivibration performance, and a high efficiency in unknown environments.

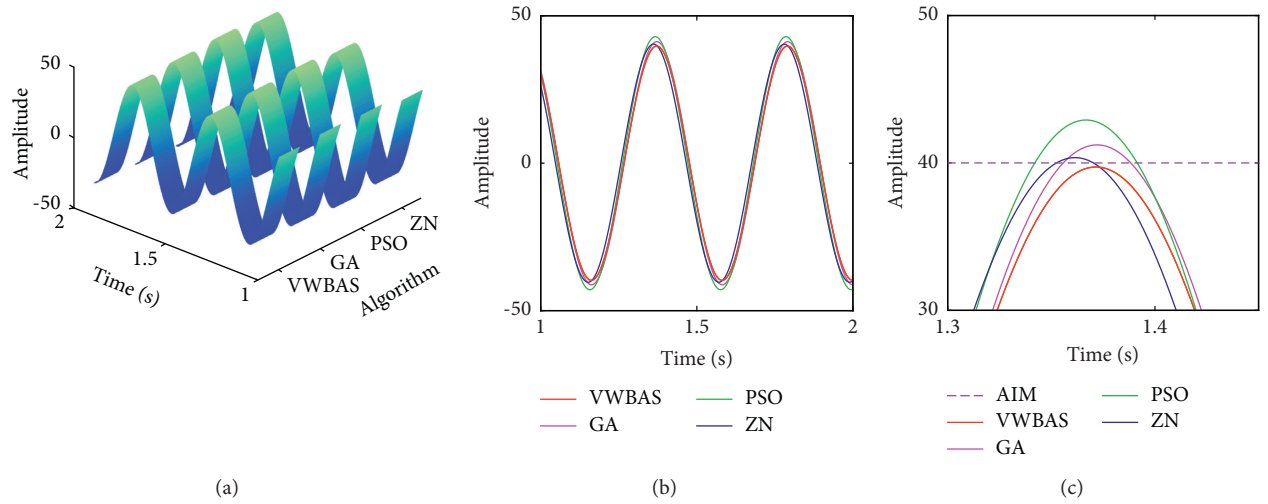

Figure 11: The frequency response of amplitude 40 and angular velocity 15: (a) three-dimension curve; (b) two-dimension curve; (c) local amplification.

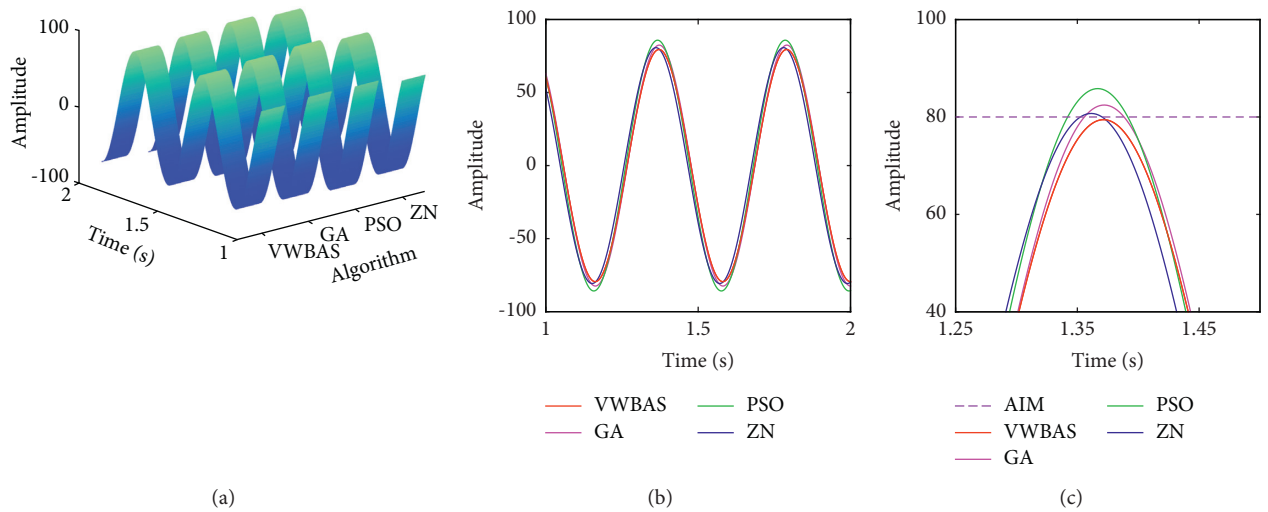

Figure 12: The frequency response of amplitude 80 and angular velocity 15: (a) three-dimension curve; (b) two-dimension curve; (c) local amplification.

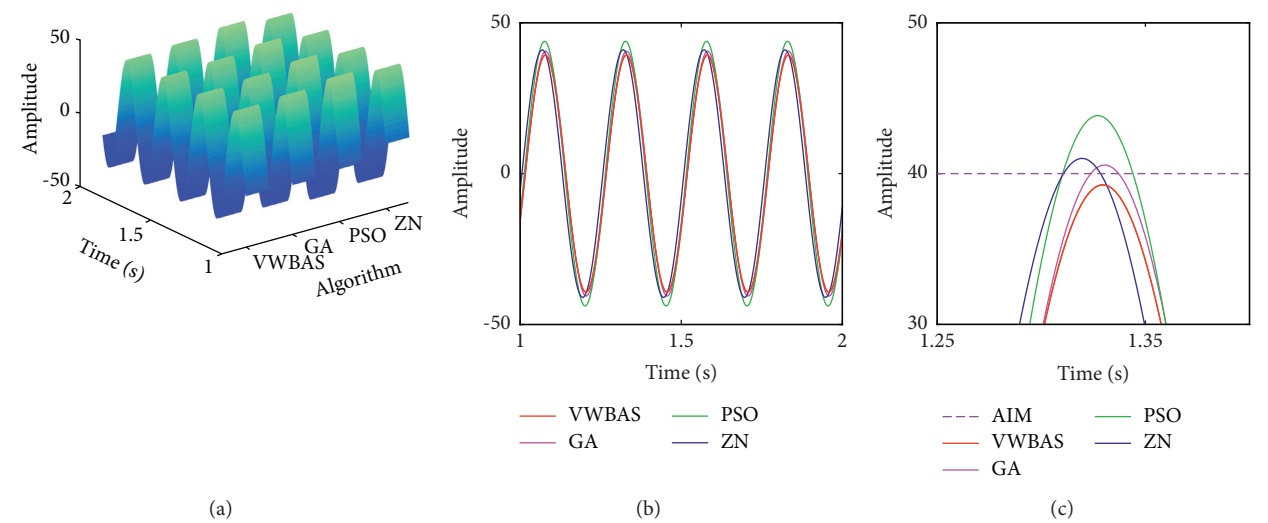

Figure 13: The frequency response of amplitude 40 and angular velocity 25: (a) three-dimension curve; (b) two-dimension curve; (c) local amplification.

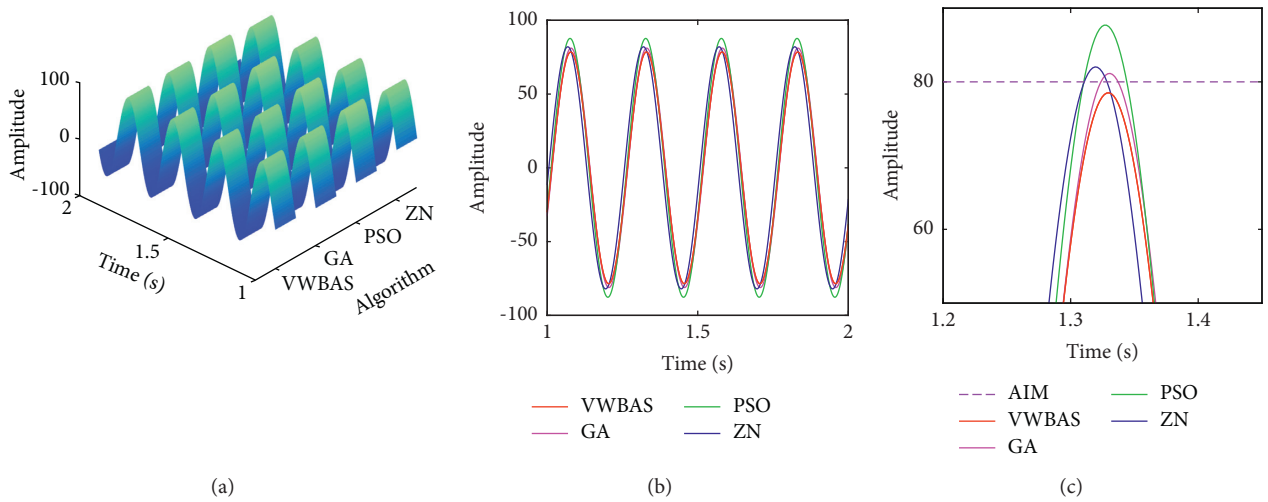

FIGURE 14: The frequency response of amplitude 80 and angular velocity 25: (a) three-dimension curve; (b) two-dimension curve; (c) local amplification.

7. Conclusions

In this paper, an enhanced beetle antennae search algorithm with variable weights (VWBAS) was introduced for selecting reasonable PID controller parameters and using the PID controller in the hydraulic system to enhance the hydraulic system performance. For VWBAS, variable weights were added to the searching procedure. To weaken the probability of being trapped in a local solution, an exponential equation was introduced, which can be declined exponentially from the difference of the searching scope. The proposed algorithm can be used to find the global optimal solution in complicated and complex problems due to its fewer selected parameters, the simplicity, and quick convergence speed. Then, different function testing experiments were carried out to show good performances of the proposed algorithm. Theoretical analysis, mathematical statistics, and experimental results show the effectiveness of VWBAS. Experiments with different testing functions reveal that the proposed algorithm can increase the efficiency of the proposed algorithm. The Wilcoxon rank-sum test result lots further reveal the superiority of VWBAS over the basic BAS. Different results for different multidimensional problems reveal the competition and superiority of the proposed algorithm. For the hydraulic system, the control system model was established. Then, the system evaluation function ITSE was selected. Finally, the temporal response characteristic and the frequency response characteristic were given in this paper. The system analysis results display that the proposed method can select reasonable PID parameters, and the designed PID controller can make the hydraulic system achieve good performances.

In the future study, we will design a new algorithm based on the basic BAS and other algorithms to enhance the searching speed and accuracy in the basic BAS. Then, we will further expand the application field of swarm intelligence algorithms and use the proposed algorithm in different industrial optimization problems. Finally, we will propose a new controller based on PID and other controllers to increase performances in the hydraulic systems.

Data Availability

The data used to support the findings of this study are available from the corresponding author upon request.

Conflicts of Interest

The authors declare that there are no conflicts of interest regarding the publication of this paper.

Acknowledgments

This research was funded by the National Natural Science Foundation of China (grant no. 51675142).

References

[1] D. Zhao, D. Li, Y. Ma, Z. Feng, and Y. Zhao, "Experimental study on methane desorption from lumpy coal under the action of hydraulic and thermal," *Advances in Materials Science and Engineering*, vol. 2018, Article ID 3648430, 10 pages, 2018.

[2] Q. Guo, Z. Zuo, and Z. Ding, "Parametric adaptive control of single-rod electrohydraulic system with block-strict-feedback model," *Automatica*, vol. 113, Article ID 108807, 2020.

[3] X. Jia, L. He, and H. Zhang, "Effect of turbine rotor disc vibration on hot gas ingestion and rotor-stator cavity flow," *Aerospace Science and Technology*, vol. 98, Article ID 105719, 2020.

[4] J. Na, Y. Li, Y. Huang, G. Gao, and Q. Chen, "Output feedback control of uncertain hydraulic servo systems," *IEEE Transactions on Industrial Electronics*, vol. 67, no. 1, pp. 490–500, 2020.

[5] L. Yang, S. Li, and X.-m. Wang, "Time-varying hydraulic gradient model of paste-like tailings in long-distance pipeline transportation," *Advances in Materials Science and Engineering*, vol. 2017, Article ID 5276431, 8 pages, 2017.

[6] Q. Guo, Q. Wang, and X. Li, "Finite-time convergent control of electrohydraulic velocity servo system under uncertain parameter and external load," *IEEE Transactions on Industrial Electronics*, vol. 66, no. 6, pp. 4513–4523, 2019.

[7] X. Jia, H. Zhang, and Q. Zheng, "Numerical investigation on the effect of hot running rim seal clearance on hot gas ingestion into rotor-stator system," *Applied Thermal Engineering*, vol. 152, pp. 79–91, 2019.

[8] B. Gao, J. Shao, and X. Yang, "A compound control strategy combining velocity compensation with ADRC of electrohydraulic position servo control system," *ISA Transactions*, vol. 53, no. 6, pp. 1910–1918, 2014.

[9] Y. Liu, G. Ye, Z. Zhao, and A. Gloria, "Prediction of hydraulic automatic transmission reliability using failure data based on exponential decay oscillation distribution model," *Advances in Materials Science and Engineering*, vol. 2021, Article ID 9424957, 22 pages, 2021.

[10] S. Zhang, S. Li, and T. Minav, "Control and performance analysis of variable speed pump-controlled asymmetric cylinder systems under four-quadrant operation," *Actuators*, vol. 9, no. 4, p. 123, 2020.

[11] Q. Guo and Z. Chen, "Neural adaptive control of single-rod electrohydraulic system with lumped uncertainty," *Mechanical Systems and Signal Processing*, vol. 146, Article ID 106869, 2021.

[12] M. Elsisi, "Optimal design of nonlinear model predictive controller based on new modified multitracker optimization algorithm," *International Journal of Intelligent Systems*, vol. 35, no. 11, pp. 1857–1878, 2020.

[13] G. Wang, B. Wang, and C. Zhang, "Fixed-time third-order super-twisting-like sliding mode motion control for piezoelectric nanopositioning stage," *Mathematics*, vol. 9, no. 15, p. 1770, 2021.

[14] Y. Li, T. Zhang, and Y. Zhang, "Adaptive control of the chaotic system via singular system Approach," *Journal of Applied Mathematics*, vol. 2014, Article ID 580105, 6 pages, 2014.

[15] M. Elsisi, K. Mahmoud, M. Lehtonen, and M. M. F. Darwish, "Effective nonlinear model predictive control scheme tuned by improved NN for robotic manipulators," *IEEE Access*, vol. 9, Article ID 64278, 2021.

[16] R. Wang, C. Tan, J. Xu, Z. Wang, J. Jin, and Y. Man, "Pressure control for a hydraulic cylinder based on a self-tuning PID controller optimized by a hybrid optimization algorithm," *Algorithms*, vol. 10, no. 1, p. 19, 2017.

[17] M. Elsisi, K. Mahmoud, M. Lehtonen, and M. M. F. Darwish, "An improved neural network algorithm to efficiently track various trajectories of robot manipulator arms," *IEEE Access*, vol. 9, Article ID 11911, 2021.

[18] M. Mavrovouniotis, C. Li, and S. Yang, "A survey of swarm intelligence for dynamic optimization: algorithms and applications," *Swarm and Evolutionary Computation*, vol. 33, pp. 1–17, 2017.

[19] M. A. Albadr, S. Tiun, M. Ayob, and F. Al-Dhief, "Genetic algorithm based on natural selection theory for optimization problems," *Symmetry*, vol. 12, no. 11, Article ID 1758, 2020.

[20] I. Boussaïd, J. Lepagnot, and P. Siarry, "A survey on optimization metaheuristics," *Information Sciences*, vol. 237, pp. 82–117, 2013.

[21] M. Elsisi and M. Soliman, "Optimal design of robust resilient automatic voltage regulators," *ISA Transactions*, vol. 108, pp. 257–268, 2021.

[22] W.-D. Chang and S.-P. Shih, "PID controller design of nonlinear systems using an improved particle swarm optimization approach," *Communications in Nonlinear Science and Numerical Simulation*, vol. 15, no. 11, pp. 3632–3639, 2010.

[23] J.-j. Xue, Y. Wang, H. Li, X.-f. Meng, and J.-y. Xiao, "Advanced fireworks algorithm and its application research in PID parameters tuning," *Mathematical Problems in Engineering*, vol. 2016, Article ID 2534632, 9 pages, 2016.

[24] M. Elsisi, "New design of adaptive model predictive control for energy conversion system with wind torque effect," *Journal of Cleaner Production*, vol. 240, Article ID 118265, 2019.

[25] X. Jiang and S. Li, "BAS: beetle antennae search algorithm for optimization problems," *International Journal of Robotics and Control*, vol. 1, no. 1, pp. 1–5, 2018.

[26] Y. Zhang and S. Li, "Convergence analysis of beetle antennae search algorithm and its applications," 2019, https://arxiv.org/abs/1904.02397.

[27] L. Liao and H. Yang, "Review of beetle antennae search," *Computer Engineering and Applications*, pp. 1–14, 2021.

[28] Q. Wu, Z. Ma, G. Xu, S. Li, and D. Chen, "A novel neural network classifier using beetle antennae search algorithm for pattern classification," *IEEE Access*, vol. 7, Article ID 64686, 2019.

[29] Y. Sun, G. Li, and J. Zhang, "Developing hybrid machine learning models for estimating the unconfined compressive strength of jet grouting composite: a comparative study," *Applied Sciences*, vol. 10, no. 5, Article ID 1612, 2020.

[30] Q. Wu, X. Shen, Y. Jin et al., "Intelligent beetle antennae search for UAV sensing and avoidance of obstacles," *Sensors*, vol. 19, no. 8, Article ID 1758, 2019.

[31] B. Du, Y. He, and Y. Zhang, "Open-circuit fault diagnosis of three-phase PWM rectifier using beetle antennae search algorithm optimized deep belief network," *Electronics*, vol. 9, no. 10, Article ID 1570, 2020.

[32] Y. Wang, Z. Chen, H. Zu, and X. Zhang, "An optimized RBF neural network based on beetle antennae search algorithm for modeling the static friction in a robotic manipulator joint," *Mathematical Problems in Engineering*, vol. 2020, Article ID 5839195, 10 pages, 2020.

[33] X. Li, Z. Zang, F. Shen, and Y. Sun, "Task offloading scheme based on improved contract net protocol and beetle antennae search algorithm in fog computing networks," *Mobile Networks and Applications*, vol. 25, no. 6, pp. 2517–2526, 2020.

[34] X. Jiang, Z. Lin, S. Li, Y. Ji, Y. Luan, and S. Ma, "Dynamical attitude configuration with wearable wireless body sensor networks through beetle antennae search strategy," *Measurement*, vol. 167, Article ID 108128, 2021.

[35] A. H. Khan, X. Cao, S. Li, V. N. Katsikis, and L. Liao, "BAS-ADAM: an ADAM based approach to improve the performance of beetle antennae search optimizer," *IEEE/CAA Journal of Automatica Sinica*, vol. 7, no. 2, pp. 461–471, 2020.

[36] Q. Fan, H. Huang, Y. Li, Z. Han, Y. Hu, and D. Huang, "Beetle antenna strategy based grey wolf optimization," *Expert Systems with Applications*, vol. 165, Article ID 113882, 2021.

[37] Q. Wu, Z. Chen, L. Wang et al., "Real-time dynamic path planning of mobile robots: a novel hybrid heuristic optimization algorithm," *Sensors*, vol. 20, no. 1, p. 188, 2019.

[38] S. Singh and S. Arora, "Butterfly optimization algorithm: a novel approach for global optimization," *Soft Comput*, vol. 23, pp. 715–734, 2018.

[39] A. H. Gandomi, X.-S. Yang, and A. H. Alavi, "Cuckoo search algorithm: a metaheuristic approach to solve structural optimization problems," *Engineering with Computers*, vol. 29, no. 1, pp. 17–35, 2013.

[40] X.-S. Yang, M. Karamanoglu, and X. He, "Flower pollination algorithm: a novel approach for multiobjective optimization," *Engineering Optimization*, vol. 46, no. 9, pp. 1222–1237, 2014.
[41] I. H. Osman, "Metastrategy simulated annealing and tabu search algorithms for the vehicle routing problem," *Annals of Operations Research*, vol. 41, no. 4, pp. 421–451, 1993.
[42] G.-G. Wang, L. Guo, A. H. Gandomi, G.-S. Hao, and H. Wang, "Chaotic krill herd algorithm," *Information Sciences*, vol. 274, pp. 17–34, 2014.
[43] S. A. Kazarlis, A. G. Bakirtzis, and V. Petridis, "A genetic algorithm solution to the unit commitment problem," *IEEE Transactions on Power Systems*, vol. 11, no. 1, pp. 83–92, 1996.
[44] M. Clerc and J. Kennedy, "The particle swarm - explosion, stability, and convergence in a multidimensional complex space," *IEEE Transactions on Evolutionary Computation*, vol. 6, pp. 58–73, 2002.